



Comment on “Zemmouri earthquake rupture zone (M_w 6.8, Algeria): Aftershocks sequence relocation and 3D velocity model” by A. Ayadi et al.

Jacques Déverchère,^{1,2} Bernard Mercier de Lépinay,³ Antonio Cattaneo,⁴ Pierre Strzeczynski,^{1,2,5} Eric Calais,⁶ Anne Domzig,⁷ and Rabah Bracene⁸

Received 3 November 2008; revised 1 February 2010; accepted 3 March 2010; published 30 April 2010.

Citation: Déverchère, J., B. Mercier de Lépinay, A. Cattaneo, P. Strzeczynski, E. Calais, A. Domzig, and R. Bracene (2010), Comment on “Zemmouri earthquake rupture zone (M_w 6.8, Algeria): Aftershocks sequence relocation and 3D velocity model” by A. Ayadi et al., *J. Geophys. Res.*, 115, B04320, doi:10.1029/2008JB006190.

1. Introduction

[1] Although often difficult to characterize, the relationship between a seismic rupture, its aftershock sequence, and cumulative subsurface or surface faulting or folding is an important challenge to modern seismology and seismotectonics. Among other benefits, it helps document fault length, slip, and magnitude relationships, reconstruct the evolution of the rupture process through historical and prehistorical times and identify the complexity of the deformation in its path toward the surface. This approach is a prerequisite to any seismic hazard assessment but is particularly difficult for faults whose surface trace projects offshore. A specific effort to identify and quantify the source parameters of large earthquakes in coastal areas is therefore needed, not only in subduction zones but also in areas of slow rate and/or diffuse deformation.

[2] *Ayadi et al.* [2008] present an analysis of the aftershock sequence that followed the 2003 May 21, M_w 6.8 Boumerdès-Zemmouri thrust event in Algeria, one of the strongest earthquakes to strike the north African coast in recent times. They propose a model of rupture reaching the surface offshore and a fault geometry based on the aftershock distribution and on correlations with 100 m resolution bathymetry data. Although we support the velocity model and hypocenter locations presented in that study, we question the interpretation of the geometry and position of the fault activated during the main event. The implications for seismic hazard in northern Algeria are significant because these parameters are

key factors for realistic ground motion prediction and earthquake hazard mitigation. Here, we discuss an alternative view of the surface extent of the Boumerdès-Zemmouri rupture, the geometry at depth of the thrust system, and its relationship to other fault systems in its vicinity. Our interpretation is consistent with the data presented by *Ayadi et al.* [2008] as well as with additional data, some unpublished, and some overlooked by the authors.

2. Surface Extent of the Seismogenic Fault and Seafloor Morphology

[3] Fault geometry toward the surface is difficult to assess from the 2003 hypocenter distribution alone since there are no aftershocks in the upper 5 km, and because aftershocks may scatter off the main rupture. Only one fault segment (B in Figure 3 III of *Ayadi et al.* [2008]) allows us to hypothesize a planar surface that best fits the hypocenter distribution. Although *Ayadi et al.* [2008] explain that the scatter of aftershocks around segment B is commonly observed for thrust fault events in the footwall block, they still use the overall distribution of hypocenters on cross sections to infer fault geometry and dip at depth. Doing so, the fault dip on segment B is consistent with independent studies of the main shock, which also find dip values in the same $45 \pm 5^\circ$ range [e.g., *Delouis et al.*, 2004].

[4] *Ayadi et al.* [2008, paragraph 31] argue that “whatever the dip taken between 40° and 50° , the fault geometry and related seismicity reaches the seafloor at a distance less than 10 km from the shoreline in the epicentral zone.” First, if the fault dips at a constant 45° angle all the way to the surface and if the main shock is at 8–10 km depth, the fault cannot reach the surface closer than 8–10 km from the coast. Second, the four cross sections of their Figure 3 III all indicate that the surface extent of a plane fitted through these hypocenters crops out at a distance between 10 and 15 km from the shoreline. Third, even considering that aftershocks scatter in the footwall, most epicenters should appear in map view to the south of the fault surface trace [*Ayadi et al.*, 2008, Figure 3 III]. However, many (~75%) of the largest aftershocks relocated by *Bounif et al.* [2004, Figure 2] occurred to the north of the fault trace reported by *Ayadi et al.* [2008, Figure 7]. In addition, many aftershocks relocated by *Bounif et al.* [2004]

¹Université Européenne de Bretagne, Brest, France.

²UMR 6538 Domaines Océaniques, Institut Universitaire Européen de la Mer, Université de Brest, CNRS, Plouzané, France.

³UMR 6526 GéoAzur, Université de Nice–Sophia Antipolis, CNRS, Valbonne, France.

⁴Laboratoire Environnements Sédimentaires, Ifremer, Centre de Brest, Plouzané, France.

⁵Now at Laboratoire de planétologie et Géodynamique, UMR 6112, Université du Maine, Le Mans, France.

⁶Department of Earth and Atmospheric Sciences, Purdue University, West Lafayette, Indiana, USA.

⁷Midland Valley Exploration, Glasgow, UK.

⁸SONATRACH Exploration, Boumerdès, Algeria.

and *Ayadi et al.* [2008] extend at least up to line Y = 12 km of the *Ayadi et al.*'s [2008] grid, i.e., at about 11 km from the coastline in the center of the rupture area (X = 24 km). We therefore conclude that the seismogenic part of the fault extends at least ~8–10 km offshore, regardless of the exact geometry of the rupture zone, which is incompatible with the faults drawn in Figure 7 of *Ayadi et al.* [2008].

[5] The question is also whether the intersection of that plane with the seafloor correlates with traces of recent activity in the morphology. The black arrows (local slope anomalies) pointed by *Ayadi et al.* as possible surface expressions of fault activity on their Figure 3 III are located in a water depth range of 700–1500 m, therefore significantly deeper than the thrust fault position drawn on their Figure 7 (line 1 on Figure 1), which is entirely located on the shelf at a depth less than 150 m. Using the same fault dip and strike as reported by *Ayadi et al.* [2008] and the scarps they identified on their grid (X, Y), we report on Figure 1 (dashed line 2) the approximate position of the closest thrust to the coast if a planar fault surface is hypothesized. The thrust assumed in this case intersects the midslope (dashed line 2) at a place significantly deeper than line 1, and where no systematic change in the morphology is detected along strike. During the MARADJA 2003 cruise, we surveyed the shelf with swath bathymetry, backscatter imagery, 2–5 kHz CHIRP echo sounder and high-resolution air gun seismics (see detailed track lines of the survey of *Domzig* [2006], *Domzig et al.* [2006], and *Dan et al.* [2009]). The MARADJA 2003 data set depicts a wedge-shaped, prograding depositional unit laterally continuous and undeformed throughout the shelf, with a maximum thickness of about 25 m, and pinching out toward the shelf edge (Figure 2). Therefore, the hypothesis of a single planar geometry from the aftershock hypocenters up to the surface, even considering the uncertainties on the plane strike and dip, does not match observations on the shelf and the margin upper slope. Consequently, one must assume that the fault dip changes toward the surface, becoming flatter in the upper 5 km, and/or that the fault is blind and transfers its cumulative deformation as folding.

3. Consistency of Proposed Fault Geometry With Other Data

[6] *Ayadi et al.* [2008, paragraph 32] argue that the model of flat ramp geometry proposed by *Déverchère et al.* [2005] “is not supported by the coastal uplift distribution [*Meghraoui et al.*, 2004].” The same argument is taken up again by *Belabbès et al.* [2009, paragraph 20]. Kinematic models of fault bend or fault propagation folding show that the area of vertical uplift is controlled by the position of the ramp [e.g., *Suppe*, 1983; *Medwedeff and Suppe*, 1997; *Bernard et al.*, 2007, and references therein]. For a main fault ramp centered below the coastline, as proposed by *Déverchère et al.* [2005], *Ayadi et al.* [2008], and *Belabbès et al.* [2009], the largest vertical coseismic uplift is expected directly above it, consistent with the observations of coastal uplift.

[7] More fundamentally, the flat ramp and splay fault interpretation of *Déverchère et al.* [2005] is actually not an interpretation of the 2003 rupture itself but of the fault system as a whole, which splits into several branches. Segments of that fault system, such as the one responsible for the

Zemmouri earthquake, may rupture individually, resulting in strain localization within the margin or the Algerian basin over the long term. GPS data collected during the 2.5 years after the rupture [*Mahsas et al.*, 2008] show that postseismic deformation resulted from shallow deformation, updip of the coseismic rupture and under the margin slope. It is thus possible that a significant part of the margin deformation in the upper 5 km occurred aseismically, either by afterslip or by soft deformation through folding.

[8] *Ayadi et al.* [2008, paragraph 32] also argue that “aftershocks located above 7 km on segments B and C of their Figure 3 do not show any change in the fault dip when compared with the deeper seismic events, as would be expected in a ramp-flat system.” Note first that because of the network position, the depth uncertainties of shallow events increase with the epicentral distance to the coastline. Second, the cross section shown on Figure 5 of *Déverchère et al.* [2005] is derived from a conversion of the seismic time profile using the mean seismic velocities expected in the upper crust: it is not a direct image of the junction of the flat and ramp. The multichannel section shown by *Déverchère et al.* [2005] (as line B, in *Ayadi et al.*'s Figure 3) shows the flat part of the fault near 4.8 s two-way traveltimes at 1500 m below sea level, which corresponds to a depth range of 4580–7100 m (using minimal and maximal velocities of sediments of 2.2 and 4.0 km/s). This places the approximate position of the ramp-to-flat transition close to the coastline and at a depth range of 4.5–7 km, which is consistent with the distribution of aftershocks, the known structure of the margin from seismic exploration, the coastal uplift and interferometric synthetic aperture radar data [*Belabbès et al.*, 2009], and the postseismic shallow afterslip detected by *Mahsas et al.* [2008] near the coastline.

[9] Finally, *Ayadi et al.* [2008, paragraph 32] argue that the flat ramp interpretation “is also inconsistent with the GPS data inversion of *Semmane et al.* [2005] or the regional moment tensor analysis of *Braunmiller and Bernardi* [2005].” This is not correct: *Yelles et al.* [2004, Figure 3] showed that the WSW trending coseismic displacements at GPS sites near the junction of faults F2 and F3 of *Ayadi et al.* [2008] required coseismic slip at depth on a SE dipping fault, as later confirmed by *Delouis et al.* [2004], then *Semmane et al.* [2005]. These GPS displacements preclude coseismic slip on fault F3, which would require a southeastward coseismic displacement of the Mitidja basin relative to the Blida thrust, 90° in azimuth from the GPS observations. In addition, postseismic displacements measured by continuous GPS reported in *Mahsas et al.* [2008] are well matched by slip on a single fault whose geometry is close to that used by *Semmane et al.* [2005] or *Delouis et al.* [2004] in their coseismic inversions. Taken together, these results show that at least fault F3, and most likely fault F2 as well, did not experience any significant coseismic or postseismic slip. The aftershocks reported in *Ayadi et al.* on those faults are more logically explained as seismicity triggered by stress changes caused by the main shock rupture, as often observed after large or moderate earthquakes (e.g., the M_w 6.5 San Simeon 2003 event [see *Hauksson et al.*, 2004]). Finally, *Braunmiller and Bernardi* [2005] propose a gentle dip ($25^\circ \pm 5^\circ$) of the rupture plane which contradicts the results of *Ayadi et al.* The aftershock relocation by *Ayadi et al.* provides extensive evidence for a fault dip of $45^\circ \pm 5^\circ$ inland in the center of the rupture (seg-

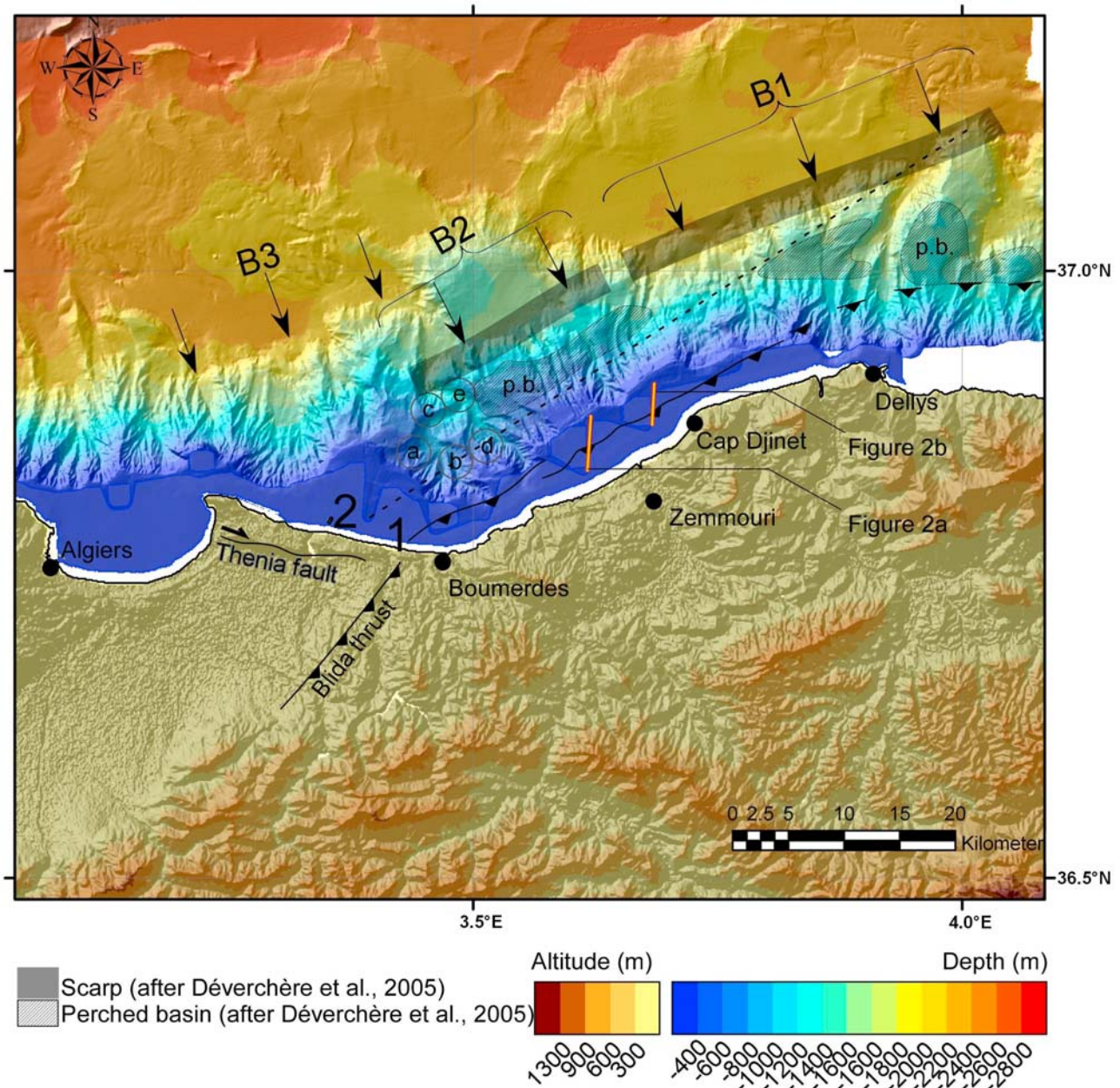


Figure 1. Map view of the different positions of the Boumerdès–Zemmouri fault trace, plotted on a 100 m DEM of the area. Line 1, position given by *Ayadi et al.* [2008]; line 2 (dashed line), position assumed using a mean dip of the fault at depth of 45° from aftershocks of segment B by *Ayadi et al.* [2008], a strike of N57°, and a constant dip up to the surface; arrows on gray shaded boxes (B1, B2), position inferred by *Déverchère et al.* [2005], *Domzig* [2006], *Domzig et al.* [2006], and *Dan* [2007] from the seafloor morphology, slide scars and depositional pattern of Quaternary sediments. Points a, b, c, d, e refer to “scarps” identified by *Ayadi et al.* [2008] on their grid and cross sections for segment B, which are supposed to coincide with the surface extension of the seismic clusters using dips of 40°–45° SE. They correspond to X and Y values of (12,12), (15,10), (15,14), (18,11) and (18,14), respectively, in kilometers (arrows on Figure 3 III of *Ayadi et al.* [2008]). However, these bathymetric anomalies do not correlate laterally to other scarps and are actually related to erosional processes on the slope (canyons and gullies). Dotted areas are flat surfaces where a perched basin (p.b.) is identified, with Quaternary growth strata thickening toward the SE [*Déverchère et al.*, 2005; *Domzig et al.*, 2006].

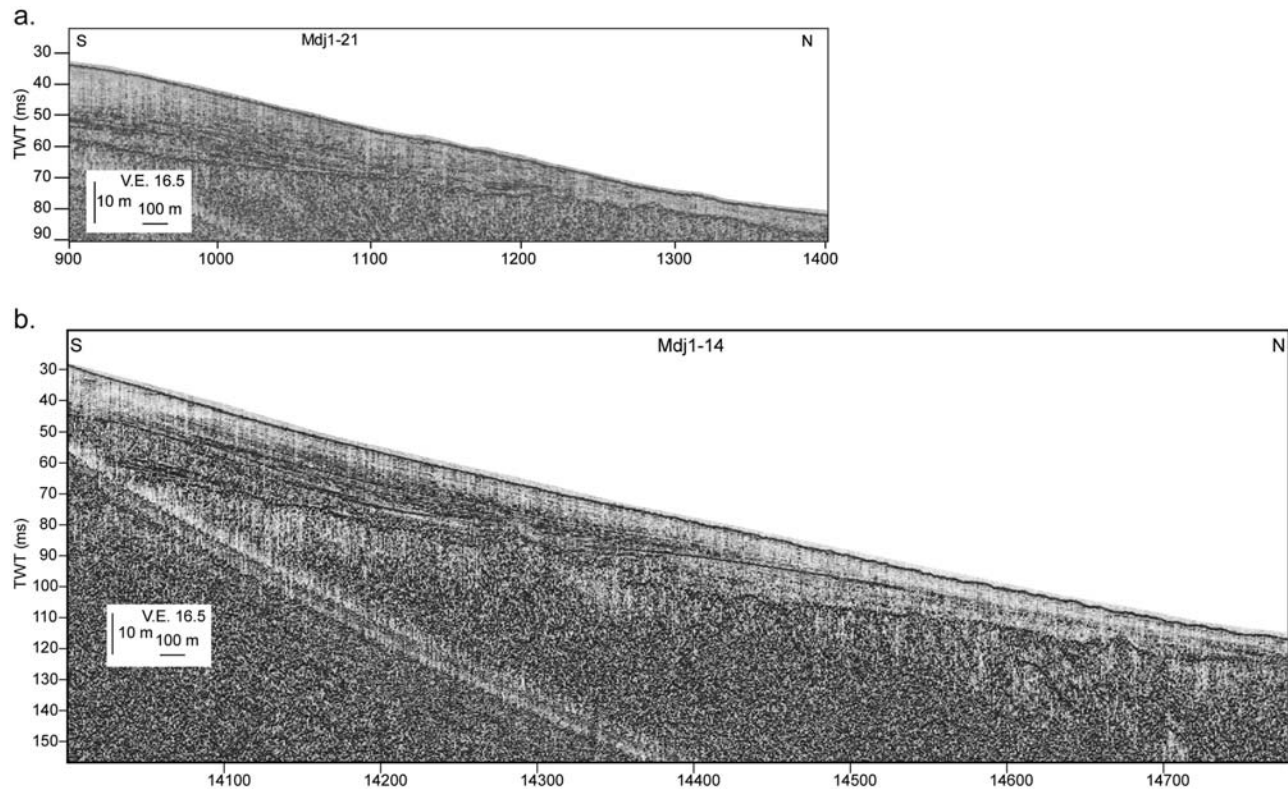


Figure 2. Typical high-resolution echo sounder (Chirp 2–5 kHz) lines across the shelf and the fault assumed by *Ayadi et al.* [2008] (see locations on Figure 1) for profiles (a) Mdj1-21 and (b) Mdj1-14. Sedimentation is basically undisturbed over more than 25 m in these two examples and depicts a progradation system above a shallow, almost flat acoustic basement. The sedimentary body forms a wedge that thins oceanward. According to preliminary results from the 2007 PRISME cruise [*Sultan et al.*, 2008], this progradation wedge represents a highstand system tract less than 7000 years old. Neither fault offset (either single or cumulative) nor local folding are observed on all the lines crossing the shelf, up to ~ 1 km from the coast. Vertical exaggeration (VE) is 16.5.

ments B and C), but does not preclude a change of dip offshore, which would explain events 5, 9, 12, 17, and 26 from *Braunmiller and Bernardi* [2005, Figure 4].

4. Relationships of the 2003 Rupture to Structures in the Seafloor Morphology and to Present-Day Depositional Systems of the Margin

[10] *Déverchère et al.* [2005] described a large morphological anomaly at the toe of the continental slope between 1600 m and 2400 m below sea level, which appears as two major slope breaks (B2 and B1) laterally continuous over ~ 22 and ~ 33 km, striking $N58^\circ$ and $N61^\circ$, respectively (Figure 1). Upslope of these scarps, a relatively flat surface, deeply incised by canyons and gullies, is observed (“RO” on Figure 4 of *Déverchère et al.* [2005]). Interestingly, these two segments coincide in length, strike and longitude with the rupture geometry as validated by leveling, seismological and geodetic data [see, e.g., *Delouis et al.*, 2004; *Yelles et al.*, 2004; *Semmane et al.*, 2005; *Ayadi et al.*, 2008]. In addition, the presence of two separate scarps B2 and B1 is consistent with the two-segment fault model (two slip patches) inferred by *Delouis et al.* [2004] and further validated by *Ayadi et al.* [2008] and *Belabbès et al.* [2009, Figure 6b]. Scarps B2 and B1 (Figure 1) are located ~ 12 km to the NW of the surface

extent of the rupture as defined by *Ayadi et al.* [2008] (line 1 in Figure 1) and ~ 7 km to the NW of its revised position from our estimate (dashed line 2 in Figure 1). We do not claim here that scarps B2 and B1 were activated during the 2003 event, nor that a flat that may connect them with the earthquake rupture slipped during the event. First, modeled coseismic slip is at most 2–3 m at depth [*Delouis et al.*, 2004] and probably about 0.5–1 m at the seafloor [*Delouis et al.*, 2004; *Belabbès et al.*, 2009], which is close to the resolution of MARADJA swath bathymetry and would hence be difficult to identify with certainty. Second, the earthquake seismic moment, well constrained from the inversion of seismological and geodetic data, is not sufficient in itself to allow for significant coseismic slip on the flat. Third, the deformation is likely to spread into a complex splay fault system that extends far inside the deep basin [*Déverchère et al.*, 2005, Figures 3 and 5], distributing the total offset over a wide area. Therefore, the transfer of slip from the 2003 earthquake rupture to the surface at the toe of the margin is probably neither instantaneous nor homogeneous or integral, and may partly result from aseismic processes [e.g., *Mahsas et al.*, 2008].

[11] The B1 and B2 cumulative scarps mapped at the toe of the continental slope are clearly very fresh and young features: they locally show meter level vertical offsets (see e.g., side-scan sonar images off Dellys canyon in the work by *Dan*

[2007]), indicative of localization of part of the deformation up to the surface and of recent tectonic activity of the fault system to which the 2003 Boumerdès–Zemmouri earthquake rupture belongs. Recent motion along these scarps is further supported by the analysis of piston cores (sampled at the foot of B2 and B1, KMDJ01 and KMDJ02 [see *Domzig*, 2006; *Dan*, 2007]) and by high-resolution bathymetric and echotype studies of the area [*Dan*, 2007; *Dan et al.*, 2009]. Both studies show that scarps B1 and B2 are systematically associated with local slides at the slope break and with sediment gravity flows overlying episodic turbidity deposits and hemipelagic deposits as young as 1400–2300 calibrated years B.P. In addition, *Déverchère et al.* [2005] identified a system of growth strata above the B1 and B2 segments that forms a narrow basin on the slope (flat surfaces noted p.b. on Figure 1), arguing for a continuous southward tilting of the strata. These geometry and disposal are typical of a basin developing by hinge migration and/or limb rotation on the hanging wall of a flat ramp structure in fault propagation or fault bend folding [e.g., *Suppe et al.*, 1992; *Storti and Poblet*, 1997; *Koyi and Maillot*, 2007].

[12] The wealth of geological and geophysical data recently acquired offshore Boumerdès is therefore consistent with the Boumerdès–Zemmouri thrust fault segments reaching the seafloor at scarps B1 and B2 (Figure 1) and with a ramp-flat geometry connecting these scarps with the 2003 earthquake rupture at depth. Uncertainties on the position of the main shock and aftershocks leave the possibility open that changes of dip of the main fault toward the surface are insignificant, if a gentler dip and a deeper and more northern rupture are combined. However, it would be very difficult to fit the main trends of hypocenters of segment B (Figure 3 III of *Ayadi et al.*) in this case, and the peculiar morphology of the margin as well as the western perched basin identified (p.b. off Zemmouri in Figure 1, located north of line 2) would remain unexplained.

5. Relations of the Boumerdès Thrust System With Structures Farther West

[13] *Ayadi et al.* [2008] show that the contact between the Blida fold and thrust system and the metamorphic Kabyle Block is underlined by a change in the seismic velocities (KF, *Ayadi et al.*'s Figure 1b) [*Ayadi et al.*, 2008, Figure 4]. This contact is a major inherited structure that accommodates the Miocene collision of the so-called “AlCaPeKa” allochthonous terranes with the African margin [e.g., *Bouillin et al.*, 1986]. Coseismic GPS [*Yelles et al.*, 2004] and coastal uplift measurements [*Meghraoui et al.*, 2004] show that the Boumerdès–Zemmouri rupture stopped abruptly near this contact, suggesting that the aftershocks observed farther west (segments F2 and F3 of *Ayadi et al.* [2008]) represent seismicity triggered by stress loading at the tip of the fault. However, *Ayadi et al.* [2008, paragraph 31] consider that “the Zemmouri earthquake occurred on the northeastern continuation of the en echelon fault system bordering the Mitidja basin to the south (Figure 1b).” First, the Miocene tectonic history recalled above precludes a direct connection between the two systems, because the Kabyle block is a large allochthonous terrane with a rheology, thermal and geological history distinct from the Blida fold and thrust system, which belongs to the External Zones of the orogenic belt. Second,

the lateral offset between the two fault systems is at least of 5 km, even considering a planar fault geometry up to the surface (Figure 1), and is more likely greater than 10 km if scarps B2 and B1 mark the cumulative surface fault trace (Figure 1). Third, the fact that the 2003 rupture stops abruptly at the contact of the two systems supports the existence of a mechanical discontinuity between them, as the much steeper dips of faults F2 and F3 also do. The question of the transfer of deformation west of the Boumerdès–Zemmouri fault remains open. On land, several other faults than the Blida thrust, as the Thenia and F2 faults [*Ayadi et al.*, 2008], the scarp B3 offshore (Figure 1), or the Reghaia fault (F7 [*Yelles-Chaouche et al.*, 2006]) may play a role in this transfer, a question that requires a quantitative study of strain and stress distribution.

6. Conclusion

[14] Taking into account submarine active faulting in seismic hazard assessment is crucial for the coastal cities of Algeria. A recently performed survey of the faulting system offshore Algeria reveals recent and active deformation of the margin [*Domzig*, 2006; *Domzig et al.*, 2006; *Kherroubi et al.*, 2009]. The work by *Ayadi et al.* [2008] provides useful new information on the distribution of aftershocks following the 2003 Boumerdès earthquake, but we show that their interpretation of the position and geometry of the Boumerdès–Zemmouri fault is not consistent with the seafloor and subsurface observations made in this area. The seismicity distribution and velocity model proposed by *Ayadi et al.* [2008] are however consistent with a flat-and-ramp geometry of the fault system. This interpretation is further supported by independent observations following the 2003 Boumerdès–Zemmouri event, in particular, the presence of seafloor escarpments and the distribution of local slide scars and gravity-driven deposits evidenced by swath bathymetry, seafloor backscatter imagery, and high-resolution seismic reflection data. In addition, the hypothesis of a fault rupture (or even an anticline) reaching the surface parallel to the coastline on the shelf and continuing onshore along the southern border of the Mitidja basin violates the available morphological, structural, seismological, and geodetic data. The ramp-flat fault system (the ramp at depth was likely the only portion to rupture coseismically during the 2003 event) proposed by *Déverchère et al.* [2005] is the best hypothesis in order to explain (1) the recent fault scarps observed at the toe of the margin ~15–17 km away from the coastline, whose geometry matches the length, strike and segmentation of the 2003 main shock, and (2) the recent depositional pattern on the lower slope, with Quaternary perched sedimentary basins continuously tilted southward, consistent with hanging wall units developing over a shallow ramp.

References

- Ayadi, A., C. Dorbath, F. Ousadou, S. Maoche, M. Chikh, M. A. Bounif, and M. Meghraoui* (2008), Zemmouri earthquake rupture zone (M_w 6.8, Algeria): Aftershocks sequence relocation and 3D velocity model, *J. Geophys. Res.*, *113*, B09301, doi:10.1029/2007JB005257.
- Belabbès, S., C. Wicks, Z. Çakir, and M. Meghraoui* (2009), Rupture parameters of the 2003 Zemmouri (M_w 6.8), Algeria, earthquake from joint inversion of interferometric synthetic aperture radar, coastal uplift, and GPS, *J. Geophys. Res.*, *114*, B03406, doi:10.1029/2008JB005912.

- Bernard, S., J. -P. Avouac, S. Dominguez, and M. Simoes (2007), Kinematics of fault-related folding derived from a sandbox experiment, *J. Geophys. Res.*, *112*, B03S12, doi:10.1029/2005JB004149.
- Bouillin, J. -P., M. Durand-Delga, and P. Olivier (1986), Betic-Rifian and Tyrhenian Arcs: Distinctive features, genesis and development stages, in *The Origin of Arcs*, *Dev. Geotectonics*, vol. 21, edited by F. C. Wezel, pp. 281–304, Elsevier, Amsterdam.
- Bounif, A., et al. (2004), The 21 May 2003 Zemmouri (Algeria) earthquake $M_w = 6.8$: Relocation and aftershocks sequence analysis, *Geophys. Res. Lett.*, *31*, L19606, doi:10.1029/2004GL020586.
- Braunmiller, J., and F. Bernardi (2005), The 2003 Boumerdes, Algeria earthquake: Regional moment tensor analysis, *Geophys. Res. Lett.*, *32*, L06305, doi:10.1029/2004GL022038.
- Dan, G. (2007), Processus gravitaires et évaluation de la stabilité des pentes: Approche géologique et géotechnique—Application à la marge algérienne et à l'effondrement de l'aéroport de Nice en 1979, Ph.D. dissertation, 458 pp., Inst. Univ. Eur. de la Mer, Brest Univ., Brittany, France. (Available at <http://tel.archives-ouvertes.fr/tel-00274695/en/>)
- Dan, G., N. Sultan, B. Savoye, J. Déverchère, and K. Yelles (2009), Quantifying the role of sandy-silty sediments in generating slope failures during earthquakes: Example from the Algerian margin, *Int. J. Earth Sci.*, *98*(4), 769–789, doi:10.1007/s00531-008-0373-5.
- Delouis, B., M. Vallée, M. Meghraoui, E. Calais, S. Maouche, K. Lammali, A. Mahsas, P. Briole, F. Benhamouda, and K. Yelles (2004), Slip distribution of the 2003 Boumerdes–Zemmouri earthquake, Algeria, from teleseismic, GPS, and coastal uplift data, *Geophys. Res. Lett.*, *31*, L18607, doi:10.1029/2004GL020687.
- Déverchère, J., et al. (2005), Active thrust faulting offshore Boumerdes, Algeria, and its relations to the 2003 M_w 6.9 earthquake, *Geophys. Res. Lett.*, *32*, L04311, doi:10.1029/2004GL021646.
- Domzig, A. (2006), Déformation active et récente, et structuration tectono-sédimentaire de la marge sous-marine algérienne, Ph.D. dissertation, 333 pp., Inst. Univ. Eur. de la Mer, Brest Univ., Brittany, France. (Available at <http://tel.archives-ouvertes.fr/tel-00144684/en/>)
- Domzig, A., et al. (2006), Searching for the Africa-Eurasia Miocene boundary offshore western Algeria (MARADJA'03 cruise), *C. R. Geosci.*, *338*, 80–91, doi:10.1016/j.crte.2005.11.009.
- Hauksson, E., D. Oppenheimer, and T. M. Brocher (2004), Imaging the source region of the 2003 San Simeon earthquake within the weak Franciscan subduction complex, central California, *Geophys. Res. Lett.*, *31*, L20607, doi:10.1029/2004GL021049.
- Kherroubi, A., J. Déverchère, A. K. Yelles, B. Mercier de Lépinay, A. Domzig, A. Cattaneo, R. Bracene, V. Gaullier, and D. Graindorge (2009), Recent and active deformation pattern off the easternmost Algerian margin, western Mediterranean Sea: New evidence for contractional tectonic reactivation, *Mar. Geol.*, *261*(1–4), 17–32, doi:10.1016/j.margeo.2008.05.016.
- Koyi, H. A., and B. Maillot (2007), Tectonic thickening of hanging-wall units over a ramp, *J. Struct. Geol.*, *29*(6), 924–932, doi:10.1016/j.jsg.2007.02.014.
- Mahsas, A., K. Lammali, K. Yelles, E. Calais, A. M. Freed, and P. Briole (2008), Shallow afterslip following the 2003 May 21, $M_w = 6.9$ Boumerdes earthquake, Algeria, *Geophys. J. Int.*, *172*(1), 155–166, doi:10.1111/j.1365-246X.2007.03594.x.
- Medwedeff, D. A., and J. Suppe (1997), Multibend fault-bend folding, *J. Struct. Geol.*, *19*(3–4), 279–292, doi:10.1016/S0191-8141(97)83026-X.
- Meghraoui, M., S. Maouche, B. Chemaa, Z. Cakir, A. Aoudia, A. Harbi, P. J. Alasset, A. Ayadi, Y. Bouhadad, and F. Benhamouda (2004), Coastal uplift and thrust faulting associated with the $M_w = 6.8$ Zemmouri (Algeria) earthquake of 21 May, 2003, *Geophys. Res. Lett.*, *31*, L19605, doi:10.1029/2004GL020466.
- Semmane, F., M. Campillo, and F. Cotton (2005), Fault location and source process of the Boumerdes, Algeria, earthquake inferred from geodetic and strong motion data, *Geophys. Res. Lett.*, *32*, L01305, doi:10.1029/2004GL021268.
- Storti, F., and J. Poblet (1997), Growth stratal architectures associated to décollement folds and fault-propagation folds: Inferences on fold kinematics, *Tectonophysics*, *282*(1–4), 353–373, doi:10.1016/S0040-1951(97)00230-8.
- Sultan, N., et al. (2008), PRISME cruise: Report and preliminary results, *Rep. IFR CB/GM/LES/08-11*, 180 pp., Ifremer, Brest, France.
- Suppe, J. (1983), Geometry and kinematics of fault-bend folding, *Am. J. Sci.*, *283*, 684–721.
- Suppe, J., G. T. Chou, and S. C. Hook (1992), Rates of folding and faulting determined from growth strata, in *Thrust Tectonics*, edited by K. McClay, pp. 105–122, Chapman and Hall, London.
- Yelles, K., K. Lammali, A. Mahsas, E. Calais, and P. Briole (2004), Coseismic deformation of the May 21st, 2003, $M_w = 6.8$ Boumerdes earthquake, Algeria, from GPS measurements, *Geophys. Res. Lett.*, *31*, L13610, doi:10.1029/2004GL019884.
- Yelles-Chaouche, A. K., A. Boudiaf, H. Djellit, and R. Bracene (2006), La tectonique active de la région nord-algérienne, *C. R. Geosci.*, *338*, 126–139, doi:10.1016/j.crte.2005.11.002.

R. Bracene, SONATRACH Exploration, Centre de Recherche et Développement, Avenue du Premier novembre, Boumerdes 35000, Algeria.

E. Calais, Department of Earth and Atmospheric Sciences, Purdue University, West Lafayette, IN 47907, USA.

A. Cattaneo, Laboratoire Environnements Sédimentaires, Ifremer, Centre de Brest, F-29280 Plouzané, France.

J. Déverchère, UMR 6538 Domaines Océaniques, Institut Universitaire Européen de la Mer, Université de Brest, CNRS, Place Copernic, F-29280 Plouzané, France. (jacdev@univ-brest.fr)

A. Domzig, Midland Valley Exploration, 144 West George St., Glasgow G2 2HG, UK.

B. Mercier de Lépinay, UMR 6526 GéoAzur, Université de Nice–Sophia Antipolis, CNRS, 250 rue Einstein, F-06560 Valbonne, France.

P. Strzeczynski, Laboratoire de planétologie et Géodynamique, UMR 6112, Université du Maine, Av. Olivier Messiaen, F-72085 Le Mans, France.